Journal of Multidisciplinary Engineering Science and Technology (JMEST)
ISSN: 2458-9403
Vol. 9 Issue 11, November - 2022

Computational Investigation Of The Effect Of A U-Tube's Cross-Sectional Shape On Its Flow And Thermal Fields' Characteristics

Christos Ziavras
Mechanical Engineering and Aeronautics Dept.
University of Patras
Patras, Greece
xri6688@gmail.com

Harris Linardos
Mechanical Engineering and Aeronautics Dept.
University of Patras
Patras, Greece
calinard@upatras.gr

Dionissios P. Margaris
Mechanical Engineering and Aeronautics Dept.
University of Patras
Patras, Greece
margaris@upatras.gr

***Abstract*—Energy crisis is a critical problem nowadays, which is creating challenging conditions in various aspects of live. To achieve energy conservation, it is important to examine solutions that can create enhanced heat transfer and less pressure drop. The U-tube is a very common type of pipe, since it is applied almost everywhere due to its ability to accommodate highly packed structures in a very limited space and utilizing the centrifugal forces for improving the flow and thermal characteristics of a system, thus lowering significantly the overall construction and operating cost. In this study, various cross sections of a U-tube are examined regarding their flow and thermal performance. More specifically, an analytical study of a circular, elliptical, rectangular and trapezoidal cross section was made, providing better comparative understanding of the phenomena taking place inside these pipes. The simulations were conducted using Ansys Fluent 2020R2 computational package, with a standard hydraulic diameter of 38mm and at Reynolds Number 10k. For the elliptical and trapezoidal cross sections, 3 and 2 respectively, alternative dimensions are offered, based on constant length ratios. The working fluid is water, entering the tubes at 298.15K and ca. 1atm, with constant wall temperature at 353.15K. The simulations showed that the circular cross section offered at the outlet the highest mean temperature and mean tangential velocity, while the elliptical cross section offered the smallest pressure drop, depending though on its orientation in space. Sharp corners caused a negative effect on heat transfer ability as well as on flow parameters.**

Keywords* — *Turbulent flow; U-tube; cross section variations; heat transfer enhancement; CFD simulations

I. INTRODUCTION

Every day that passes by it is becoming more and more obvious that there is an increasing need to maximize the heat transmission between the walls of a pipe and the fluid running inside in various applications. The reasons behind this increasing need are arising from various aspects of everyday life. Energy crisis has become a significant global matter, especially after the geopolitical issues that the war in Ukraine created. Also, global warming is creating serious and continuous problems, while heat transfer plays a vital role in CO2 emission reduction and energy saving. This becomes clear if we mention that approximately 20–50% of the energy input in industries at the United States is lost as waste heat [1]. All these factors, combined with the problems that the pandemic of COVID-19 created -basically on the economic aspects- make the efficiency of heat transfer on piping systems very important, as there is no room for loss and overuse of energy, with the demand for power constantly increasing.

Piping systems can be found in various applications. They are used from smaller applications such as water supply systems in houses and can be expanded in much more complex applications like natural gas piping, combustion chambers, heat exchangers and cooling of chemical reactors. It can also be mentioned that there is use even in physiology, as these geometries contribute in better understanding of the flow in blood vessels and therefore help in the prevention and cure of such health problems. [2]

Curvature in a pipeline can resolve various problems, with the most important being the fact that it can fit in many geometries and so solve important geometrical problems. Another great characteristic of the curvature is that it helps enhance heat transfer rate h (or Nu), because of the extended mixing happening -deriving from the development of secondary flow- as the flow becomes turbulent. Additionally, bending across a tube can raise the velocity to higher values. At the same time there are issues accompanying the curvatures such as pressure drop and vorticity -creation of symmetrical eddies, called Dean vortices [3]- in comparison to the straight pipes.

In order to study the advantages that curved pipes produce in heat transferring it is important to understand the way it is succeeded. There are many heat transfer techniques, but the most commonly applied is convective heat transfer. It is divided into two distinct categories, active and passive. Active techniques require the use of external power to increase heat transfer rate, while passive techniques do not involve external input, such as electrical power or mechanical actuation to operate. [4] The second ones rely on altering the imposed geometry with enhancements such as twists, fins and bends. In this study the effect of centrifugal forces exercised in the fluid was taken advantage of with bending across the tube. These techniques are used frequently as they provide low-cost solutions, without changing the already applied technologies. So, there is an increasing need to maximize the understanding of them, to generate efficient and low-cost heat transmission between the walls of the pipes and the passing fluid. More specifically, in this study, U-bend and multiple cross sections were utilized to augment the heat transfer across the tube.

When it comes to curved pipes one of the first works is that of Dean [3] [5] who was the first to acknowledge the vortices -now known as Dean vortices- created inside the bend and like White [6] generally studied the morphology of the flow because of the curvature. Later, J. Azzola et al. [7] extended previous works to U-tubes and the effects in the bend and downstream, with the conclusion that k-e eddy viscosity model is more adequate to such flows. Also, Ohadi et al. [8] studied the mass transfer downstream an 180° pipe and the appearance of the effect of laminarization after the bending. They concluded that the extent of laminarization depends on the extent of run of the flow in the curved element and on the magnitude of the Reynolds number. The longer the length of run, the greater the expected degree of laminarization and additionally, lower Reynolds number at the inlet, produces more susceptible flow to laminarization. The same effect was studied by M. Kurokawa et al. [9] who confirmed the stabilizing of the flow near the inner wall and the destabilizing effect near the outer wall of the 180°, by measuring the turbulence intensity and the fluctuating velocity.

Later, more studies on the curvature effects and specifically on the heat transfer enhancements it can produce, were conducted. K. Sudo et al. [10] studied the effects on 180° bends for a curvature radius ratio of 4.0. He established a better understanding of the weakening of the secondary flow starting at about 90° and the shift of the high velocity region at the outer wall in the bend exit, while the turbulence intensity still remains in the core of the bend. X. Guan & T. B. Martonen [11] simulated the U-tube flow and concluded that in the region of developing flow, after the exit of inlet part, the isovelocity contours change their shapes with θ.

Pawar et al [12], compared U-tube, helical and spiral coils with the same length proving that U-tube shows maximum variation at the outlet temperature contour, as heat absorbed from hot water is not evenly distributed in the flowing water. Additionally, Cvetkovski [13] while studying the ground source and surface water heat pumps and the effects of Reynolds and Dean number on U-tubes, concluded that heat transfer takes place mostly on the curved part of the tube. Also, Dean number has a greater effect on heat transferring than the Reynolds number. Furthermore, A Miloud et al. [14] studied the characteristics of velocity in various cross sections of the U-tube stating a pattern for the flow velocity before and after the 90° bend. M. Ayad Ali [15] simulating the U-tube flow concluded that decreasing the curvature radius ratio can increase the heat transfer coefficient and friction factor. That means that pressure losses in the curvature created by friction and momentum exchanges appear, because of the direction of the flow.

While studying curved pipes with elliptical cross section, Dean [5] and White [6] established some of the first studies on a non-circular pipe. Later, N. Tran et al [16] studied various cross sections on pipes concluding that the thermal performance of an elliptical tube is better than that of a circular tube. Moreover, they concluded that the thermal performance of an elliptical tube with a larger ratio γ, outperforms the one with a smaller ratio. Also, A. Gogolin et al [17] studied oval-like cross sections that emerged from bending a straight circular pipe and found that this shape is creating higher velocities along with higher pressure drop values.

However, to the best of our knowledge most studies on pipes with elliptical cross section focus on the laminar flow, something that is validated by [18]. So, there is an increasing need of studying this geometry with turbulent conditions along the curvature.

I. GEOMETRIES

In Figure 1 we can see analytical pictures of the proposed geometries concerning the U-tubes that will be used in our study. These geometries consist of:

- a circular model (1)
- two elliptical models with the big axis on radial direction (2)
- three elliptical models with the big axis on z direction (3)
- two trapezoidal models (4)
- a rectangular model (5)

The geometrical characteristics of the various models introduced are found in Table1.

Additionally, in Table 2 the various models are named, in order to create a better way of mentioning every model used. Finally, we created names for the 5 elliptical models (E1 - E5) and the 2 trapezoidal models (T1 – T2).

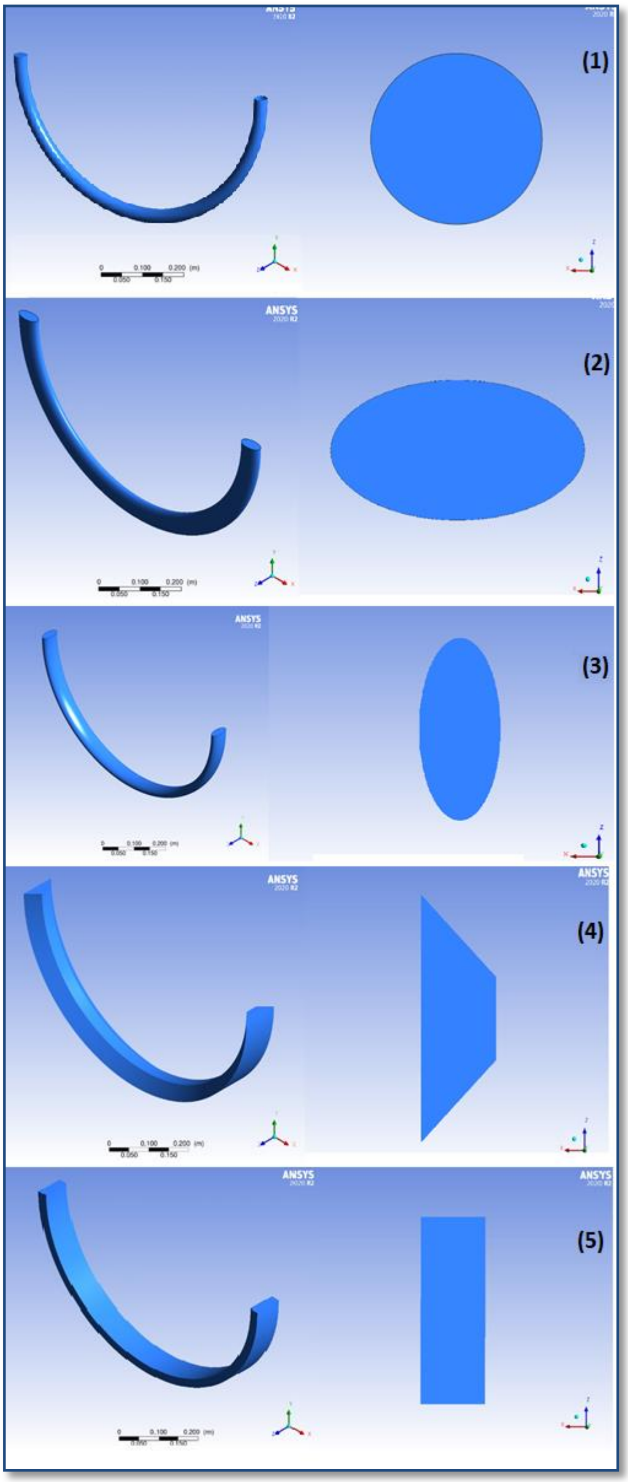

Figure 1: 3D view and corresponding cross section view of (1) Circular U-tube, (2) Elliptical U-tube with big radius on radial axis, (3) Elliptical U-tube with big radius on z-axis, (4) Trapezoidal U-tube, (5) Rectangular U-tube.

II. GOVERNING EQUATIONS

The current study is solved as a three-dimensional incompressible steady flow and heat transfer numerical simulation. The problem is solved using the continuity, momentum and energy equations, as follows [19]:

A. *Continuity equation*

$$\frac{\partial \rho u_i}{\partial x_i} = 0 \tag{1}$$

TABLE I. CHARACTERISTICS OF THE GEOMETRIES OF THE U-TUBE MODELS STUDIED.

Geometry Characteristics			
Reynolds Number		**Inlet Velocity (m/s)**	
10000		0.277	
U-tube Radius (mm)		**Hydraulic diameter (mm)**	
380		38	
(1) Circular			
Radius (mm)			
19			
(2) Elliptical			
a = R/r	**Big Radius R (mm)**	**Small Radius r (mm)**	
2	30	15	
3	42.4	14.1	
4	55.2	13.8	
(3) Trapezoidal			
a = B/b	**Big Base B (mm)**	**Small Base b (mm)**	**Height (mm)**
3	97.5	32.5	32.5
6	201	33.5	33.5
(4) Rectangular			
a = B/b	**Base B (mm)**	**Height b (mm)**	
3	75.9	25.3	

TABLE II. NAMING OF THE COMPUTED MODELS.

Models Naming		
Elliptical with big radius on radial axis [geometry (2) from figure 1]		
E1	***E2***	
a = R/r =2	a = R/r = 4	
Big Radius R = 30mm	Big Radius R = 55.2 mm	
Small Radius r = 15 mm	Small Radius r = 13.8 mm	
Elliptical with big radius on z axis [geometry (3) from figure 1]		
E3	***E4***	***E5***
a = R/r = 2	a = R/r = 3	a = R/r = 4
Big Radius R = 30mm	Big Radius R = 42.4mm	Big Radius R = 55.2 mm
Small Radius r = 15 mm	Small Radius r = 14.1mm	Small Radius r = 13.8 mm
Trapezoidal [geometry (4) from figure 1]		
T1	***T2***	
a = B/b = 3	a = B/b = 6	
Big Base B = 97.5mm	Big Base B = 201mm	
Small Base b = 32.5mm	Small Base b = 33.5mm	

B. *Momentum equation*

$$\frac{\partial(\rho \bar{u}_i \bar{u}_j)}{\partial x_j} = -\frac{\partial \bar{P}}{\partial x_i} + \frac{\partial}{\partial x_j}\left(\mu\left(\frac{\partial u_i}{\partial x_j} + \frac{\partial u_j}{\partial x_i}\right)\right) - \frac{\partial(\rho \overline{u'_i u'_j})}{\partial x_j} \tag{2}$$

C. Energy equation

$$\frac{\partial}{\partial x_i}\left(u_j(\rho e + P)\right) = \frac{\partial}{\partial x_j}\left(\kappa \frac{\partial T}{\partial x_j}\right) \tag{3}$$

with i, j = x, y, z

III. Boundary Conditions

The working fluid is liquid water, which enters the U-tube at a temperature of 298.15K and has a constant temperature of 353.15K at the wall. The Reynolds number is estimated at 10000, in order to achieve turbulent flow, with an inlet velocity of 0.277 m/s. At inlet, the hydraulic diameter is set to 0.038m, with the turbulent intensity at 5%. The selected material was aluminium.

IV. Thermophysical Properties

To achieve more accurate results, the properties of the working fluid (liquid water) weren't considered constant, but were changing as a piecewise-linear function between 298.15K and 353.15K. These properties were adopted for: density, thermal conductivity, specific heat capacity and dynamic viscosity of liquid water.

V. Numerical Investigation

The calculations in this study were carried out by the ANSYS Fluent software (2020R2 edition). Ansys discretizes and solves the governing equations with the finite volume method. The convergence criterion was set for all the residuals at 1e-06, to achieve maximum precision.

For the setup of the model runs, the Realizable k-ε model was chosen for the turbulent flow, as it treats locally transitional flows with swirling and vortices suitably. Additionally, the Enhanced Wall Treatment was selected to give more accurate resolution at the walls. For the Enhanced Wall Treatment, a y+ lower than 5 is needed. In these models the meshing is done with the goal of achieving y+ = 1.

After solving the y+ equation, a boundary layer at around 5mm seemed appropriate. This was validated by solving the finest model with 2.5 million elements and creating a chart of the axial velocity at 90° bend. In this chart, a boundary layer close to 0.5 mm seemed a good approach and so was used later on for discretization.

VI. Grid Independence Analysis

In order to establish the best possible meshing grid that provides good element quality, low skewness and low computational power, a stability analysis for the proposed geometry needs to be made. More specifically, 3 models regarding the circular cross section were proposed with similar meshing grids but increasing element numbers.

Some important information about the meshing techniques used for the 3 models can be seen in Table 3.

TABLE III. Comparison of the 3 meshing grids used for the grid independence analysis.

Meshing Comparison			
	0.7 Million Elements Model	1.5 Million Elements Model	2.5 Million Elements Model
General			
Element Size	0.0025 m	0.002 m	0.0015 m
Inflation			
Maximum Thickness	0.005 m	0.005 m	0.005 m
Number of Layers	5	10	10
Growth Rate	1.2	1.2	1.2
Edge Sizing			
Number of Divisions	100	120	150

After solving the models, with the exact same setup, the mean pressure in the same cross section of the models was calculated and a diagram was created to see if there is any convergence between the 3 models, as we can see in Figure 2.

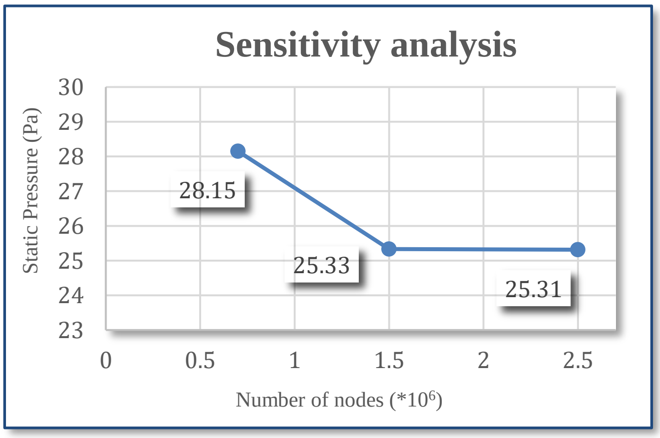

Figure 2: Grid independence analysis.

It appears there is clear convergence between the medium and fine model and the solution is normalized after 1.5 million elements. It can be concluded that using the medium model provides good results (less than 0.07% divergence between fine and medium meshing) with less elements and so less computational time needed.

Concluding, this means that the models that will be used later on our analysis will have about 1.5 million elements, without harming the precision of the calculations, while keeping hydraulic diameter the same.

VII. Discretization of Computational Domain

It is very important, especially in the circular and elliptical cross sections, to apply a suitable mesh in order to solve the boundary layer. A minimum element quality at 0.1 was set, in order to improve precision. All models were discretized with a number of about 1.5 million elements, as the grid independence analysis indicated. Edge sizing, inflation and multizone with prisms and tetra/pyramid order was used in most models, as can be seen in the pictures of Figure 3.

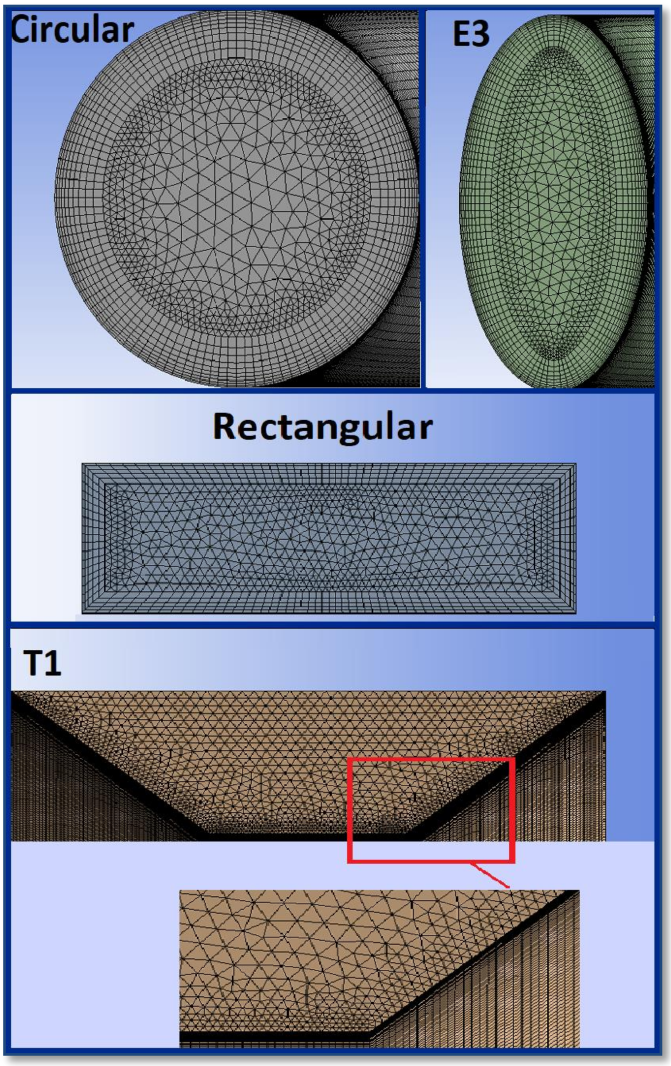

Figure 3: Circular, Elliptic E3, Rectangular and Trapezoidal T1 models meshing face.

Figure 3 gives a good understanding of the meshing used in the models, with the circular, elliptical and rectangular having a similar approach and the trapezoidal having a very finite meshing at the boundaries because of the sharp corners.

VIII. Results and Discussion

After solving all the models, the results were numerous and many observations could be made.

A. Temperature Results

The mean temperature at the outlet of every U-tube, for all the models, can be seen at Table 4.

TABLE IV. Mean temperature at the outlet cross sections of the U-tube.

Bulk Temperature Outlet		
	T (K)	***Difference from max Tout (%)***
Circular	309.25	0
E1	309.04	0.07
E2	308.54	0.23
E3	308.38	0.28
E4	308.27	0.32
E5	307.94	0.43
T1	308.36	0.29
T2	307.44	0.59
Rectangular	308.49	0.25

The evolution of the mean temperature, across the U-tube is shown in the diagram of Figure 4, for the most effective geometry of every cross section shape. It is evident that the Circular and E1 model are superior in heat transfer and must be selected in such applications.

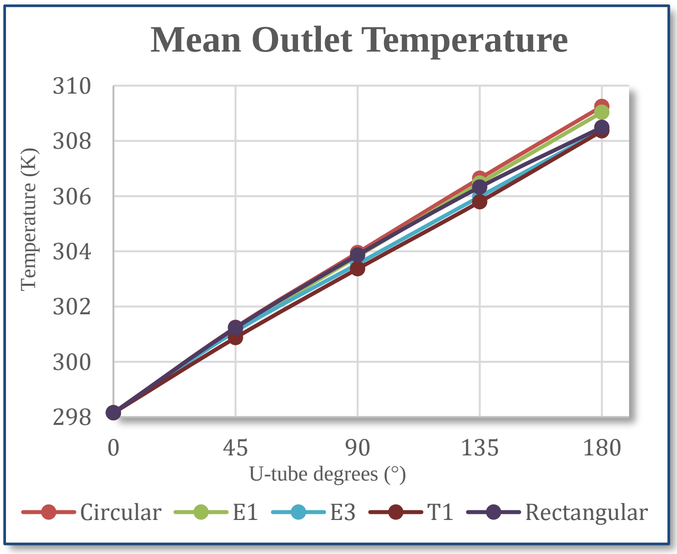

Figure 4: Evolution of the mean temperature across the U-tube for the most effective models of each cross section shape.

The corresponding contours for the temperature at the outlet cross section of each shape of U-tube can be seen at Figure 5.

The morphology of the temperature allocation of the Circular U-tube, which is the most studied, is confirmed by the already existing bibliography.

We can also observe that models E3, E4 and E5 distribute heat evenly across their cross section, while having smaller outlet temperatures. At the same time the E1, E2 and Circular model have significant temperature deviation between the inner and outer part of the U-tube. However, they can create bigger maximum temperatures overall.

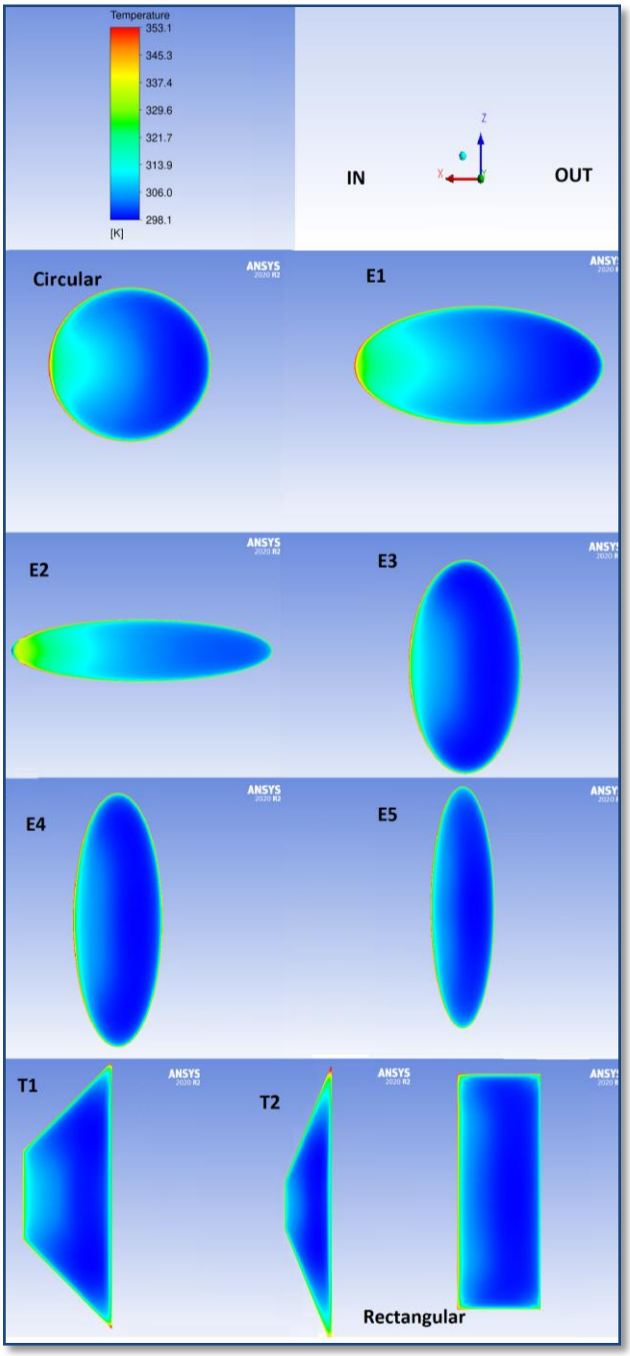

Figure 5: Temperature contours of the outlet cross section at the U-tube models.

The difference in the outlet temperature of every cross section from the most effective computed model (Circular with 309.25K) can be seen in Figure 6.

It is clear that the trapezoidal models have the worst thermal behavior, whilst the elliptical models - especially in the direction that E1 and E2 models have- are close to the effectiveness of the circular model.

As the corners in the geometries get sharper, the thermal effectiveness drops for the U-tube, while bigger angles, like rectangular and E3 and E4, have better thermal behavior.

All the geometries that approach the circular one, can achieve bigger outlet temperatures, as it appears in Figure 6.

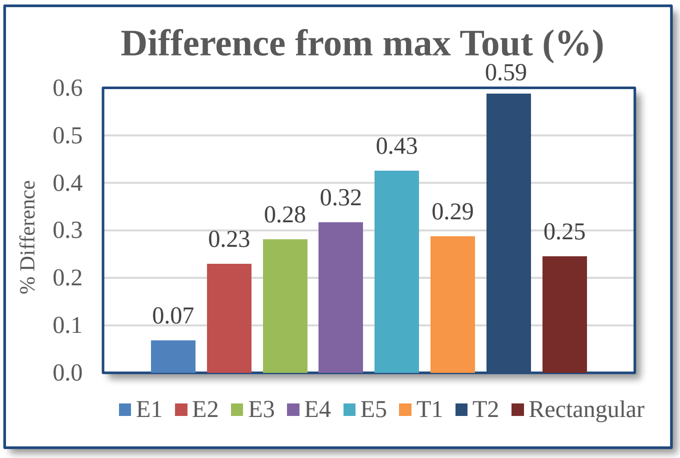

Figure 6: % Difference from maximum (Circular U-tube) outlet temperature.

B. Static Pressure Results

Static Pressure results in different angles for the U-tube were computed. The mean pressure losses at the outlet of the U-tubes can be seen in Table 5.

TABLE V. MEAN STATIC PRESSURE DROP AT THE OUTLET OF THE U-TUBE.

Mean Static Pressure		
	ΔP average (Pa)	***Difference from circular (%)***
Circular	40.92	0
E1	47.89	+14.6
E2	47.97	+14.7
E3	36.76	-11.3
E4	39.48	-3.6
E5	37.78	-8.3
T1	45.60	+10.3
T2	43.39	+5.7
Rectangular	43.22	+5.3

The difference between the models can be better interpreted with Figure 7. This diagram shows the models with the best and worst behavior regarding the mean pressure drop at the outlet.

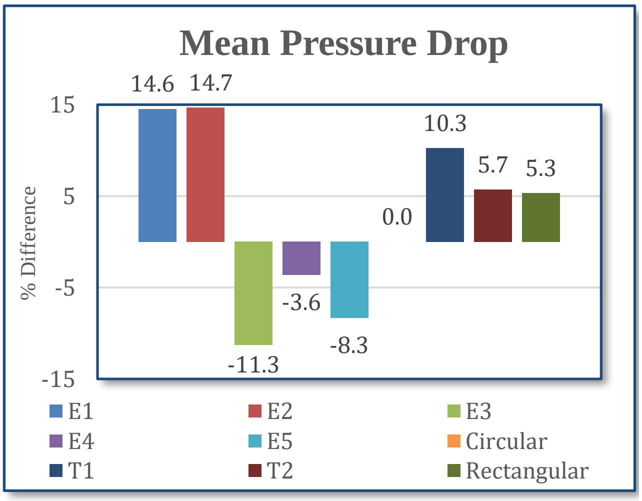

Figure 7: % difference of the pressure losses regarding the static pressure of the circular model.

The circular model has an average pressure behavior, compared to the other U-tubes. The biggest pressure drop values appear for the elliptical models E1 and E2, which have about the same results. The smallest drop in pressure is given by the elliptical models with big radius on z-axis. The E3 model has 11.3% less pressure drop compared to the circular, making it a great choice for applications with low pressure drop demands.

Once again, the trapezoidal models along with the rectangular model, have significant pressure drop across the U-tube.

Additionally, the corresponding diagram of the mean static pressure losses, computed in various angles across the U-tube, is shown in Figure 8.

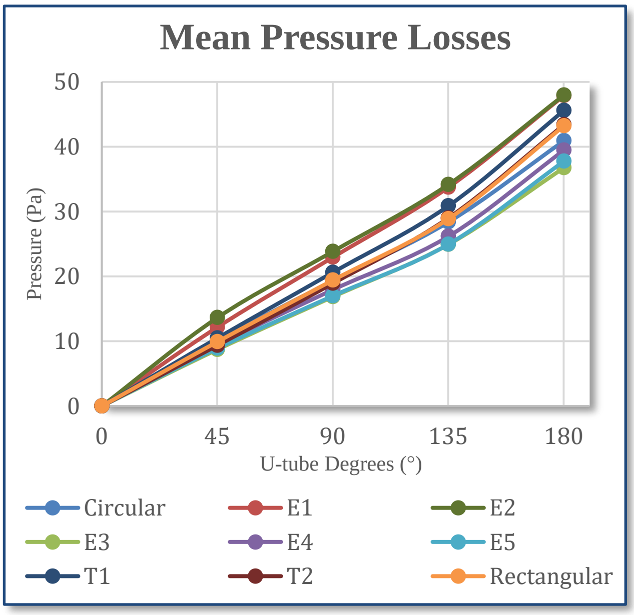

Figure 8: Mean pressure losses (ΔP) across the U-tube.

Moreover, the contours of the static pressure of all the U-tube models can be seen in Figure 9.

The biggest pressures computed are in the outer part of the U-tube for every model. At the same time, the inner part shows significantly lower pressure values. The E3, E4 and E5 contours verify that they have the best pressure behavior, as the blue part (low pressures) extends in the biggest part of the outlet, unlike models E1 and E2, which have bigger variations across the outlet.

A. Velocity Results

The results of the mean velocity computed in the 90° and 180° cross section of every U-tube are gathered in Table 6. In this table, it is evident that the circular model can achieve the biggest outlet velocity, while the E1 and E2 models accelerate the velocity faster, having the maximum velocities at 90 degrees.

The E1 model increases the velocity quicker and also achieves the second biggest outlet velocity. So, it can be concluded that it has the best overall performance in respect to velocity behavior.

Again, trapezoidal models have the worst behavior, with the corners creating parts of low velocity, decelerating the average velocity.

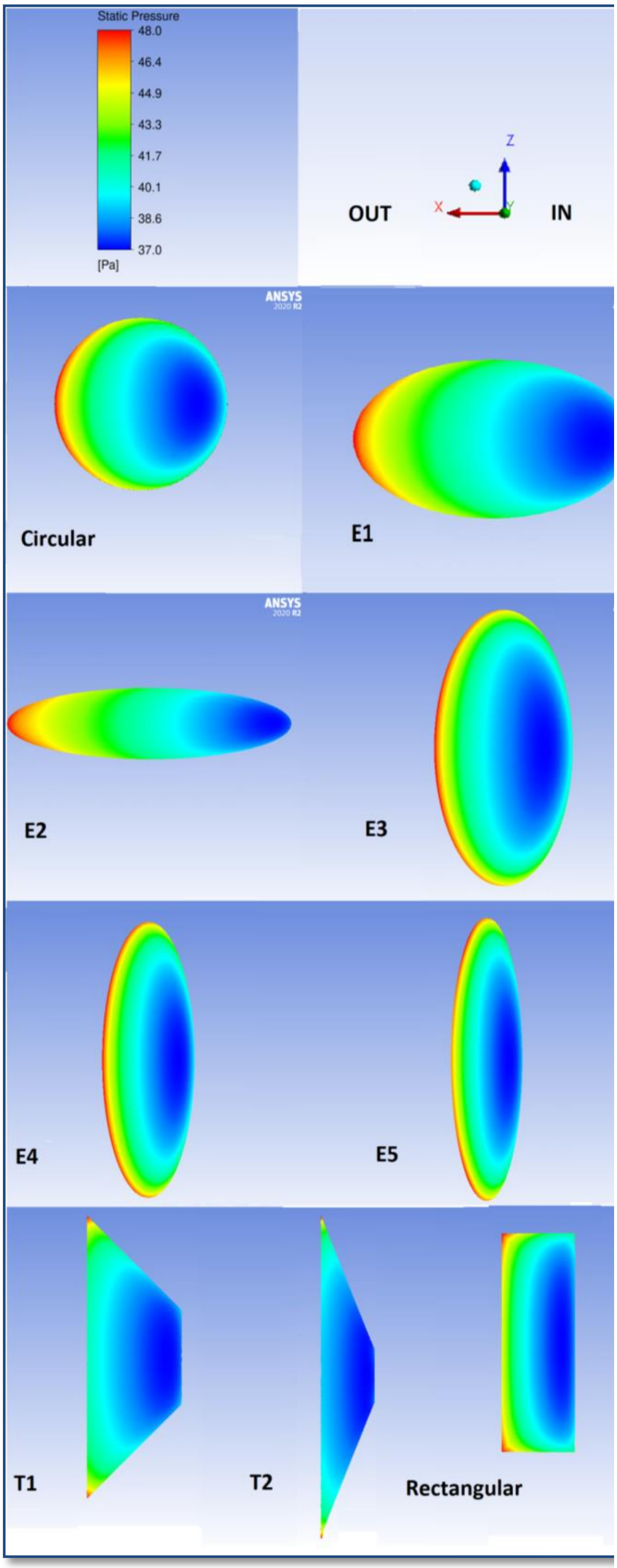

Figure 9: Mean Static Pressure contour at the outlet of the U-tube for every model.

TABLE VI. TANGENTIAL VELOCITY OF THE U-TUBE MODELS ON 90° AND 180°.

Mean Tangential Velocity		
	*Velocity 90° *10^{-3} (m/s)*	*Velocity 180° *10^{-3} (m/s)*
Circular	277.75	278.45
E1	277.82	278.42
E2	277.87	278.34
E3	277.65	278.31
E4	277.63	278.29
E5	277.63	278.25
T1	277.70	278.30
T2	277.66	278.17
Rectangular	277.72	278.36

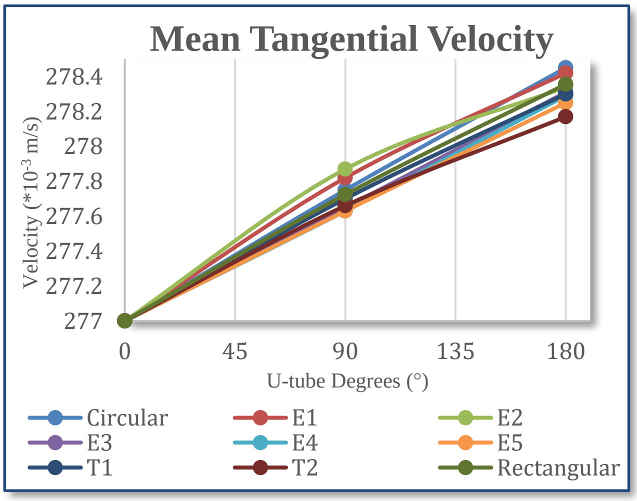

Figure 10: Mean tangential velocity across the U-tube for each geometry.

The evolution of the mean velocities from inlet, at 0.277 m/s, to the outlet can be seen in Figure 10.

The morphology of the velocity distribution for each model at the outlet can be seen in the contours of Figure 11, for every geometry imposed on the U-tube cross section.

IX. CONLUSIONS

The study of 4 shapes (circular, elliptical, rectangular and trapezoidal) of the cross section of a U-tube, encompassing dimensional and orientation variations for the two of them, has provided significant understanding on how the flow interacts with each geometry. The most important conclusions are the following:

A. The circular cross section has superior behavior regarding the heat transfer ability, as it can provide the highest mean outlet temperatures of all cross sections.

B. The elliptical cross section with radius ratio of 2 and oriented with its major axis perpendicular to U-tube's plane (model E3), produces the smallest static pressure drop at the outlet, smaller than the same cross section with transverse orientation of its major axis in space (models E1 & E2). That means the orientation in space of a U-tube's cross section will affect the flow field in terms of pressure losses.

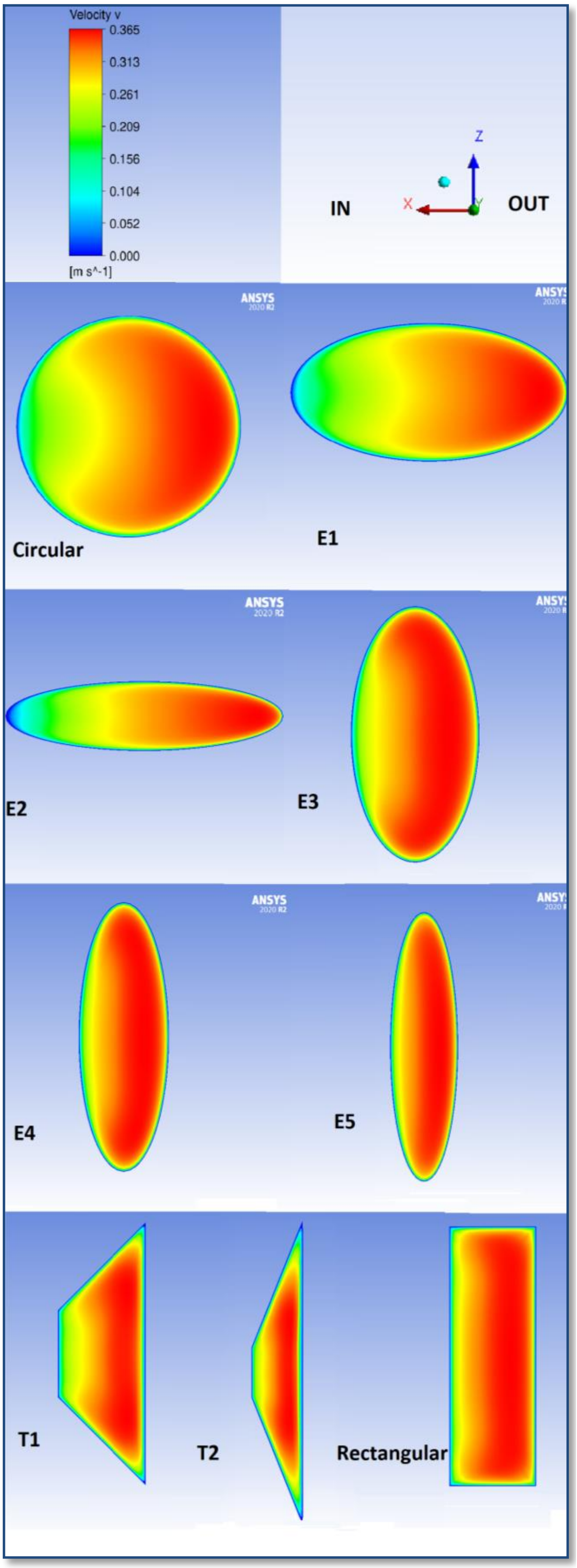

Figure 11: Velocity contours at the outlet of the U-tube

C. Even though the circular cross section produces the highest mean tangential velocity increase at the outlet, the elliptic cross section with radius ratio of 2 and major axis parallel to U-tube's plane (model E1) can reach its peak value increase much closer to U-tube's entrance, offering at the same time the highest mean tangential velocity increase across its path.

D. Sharp corners, either in rectangular or in trapezoidal cross-sections (models T1 & T2), create adverse effects on all flow and thermal aspects studied, with deteriorating effects as the angles become smaller. The regions close to the corners create stagnant or slow moving areas of the fluid, downgrading its thermal and flow interaction with pipe's walls, thus eliminating the benefits the curvature of a pipe produces.

E. Elliptic cross sections with major axis perpendicular to U-tube's plane (models E3, E4 and E5) produce the most uniform flow (velocity) and thermal (temperature) fields on each cross section, across the entire U-tube area.

F. The symmetry in a cross section's shape is proven to produce the best heat transfer enhancement as well as the highest velocity increase, while this is clearly not the case for the pressure losses.

X. Acknowledgments

The part of this research conducted by Mr. Harris Linardos was co-financed by Greece and the European Union (European Social Fund-ESF) through the Operational Programme «Human Resources Development, Education and Lifelong Learning» in the context of the Act "Enhancing Human Resources Research Potential by undertaking a Doctoral Research" Sub-action 2: IKY Scholarship Programme for PhD candidates in the Greek Universities».

XI. References

[1] M. H. Mousa a, N. Miljkovic, K. Nawaz (2021) "Review of heat transfer enhancement techniques for single phase flows," Renewable and Sustainable Energy Reviews, vol. 137, issue C, p. 11056.

[2] J. H. Siggers and S. L. Waters (2005) "Steady flows in pipes with finite curvature," Physics of Fluids, vol.17, issue 7, p. 077102.

[3] W.R. Dean (1927) "XVI. Note on the motion of fluid in a curved pipe," The London, Edinburgh, and Dublin Philosophical Magazine and Journal of Science, vol. 4, no. 20, pp. 208-223.

[4] M. Awais, A. A. Bhuiyan (2018) "Heat transfer enhancement using different types of vortex generators (VGs): A review on experimental and numerical activities," Thermal Science and Engineering Progress, vol. 5, pp. 524-545.

[5] W.R. Dean (1928) "LXXII. The stream-line motion of fluid in a curved pipe (Second paper)," The London, Edinburgh, and Dublin Philosophical Magazine and Journal of Science, vol. 5, issue. 30, pp. 673-695.

[6] C. M. White (1929) "Streamline Flow through Curved Pipes," Proceedings of the Royal Society A:

Mathematical, Physical and Engineering Sciences, vol. 123, issue 792, pp. 645-663.

[7] J. Azzola, J. A. C. Humphrey, H. Iacovides, B. E. Launder (1986) "Developing Turbulent Flow in a U-Bend of Circular Cross-Section: Measurement and Computation" Journal of Fluids Engineering, vol 108, issue 2, pp. 214-221.

[8] M. M. Ohadi and E. M. Sparrow (1990) "Effect of a 180° bend on heat transfer in a downstream positioned straight tube," International Journal of Heat and Mass Transfer, vol. 33, issue 6, pp. 1359-1362.

[9] M. Kurokawa, K. C. Cheng, L. Shi (1998) "Flow Visualization of Relaminarization Phenomena in Curved Pipes and the Related Measurements," Journal of Visualization, vol. 1, issue 1, pp. 9-28.

[10] K. Sudo, M. Sumida, H. Hibara (2000) "Experimental investigation on turbulent flow through a circular-sectioned 180° bend," Experiments in Fluids, vol. 28, issue 1, pp. 51-57.

[11] X. Guan & T. B. Martonen (1997) "Simulations of Flow in Curved Tubes," Aerosol Science and Technology, vol 26, issue 6, pp. 485-504.

[12] S. S. Pawar, H. Kolte, S. Bhalerao, V. Kakad, S. Kharat (2018) "Comparison of experimental heat transfer parameters for U-tube spiral, & helical coils of same length with CFD result," International Journal of Advance Engineering and Research Development, vol. 5, issue 4, pp. 2462-2469.

[13] C.G. Cvetkovski, S. Reitsma, T. Bolisetti, D.S.K. Ting (2015) "Heat transfer in a U-Bend pipe: Dean number versus Reynolds number," Sustainable Energy Technologies and Assessments, vol. 11, pp. 148-158.

[14] A. Miloud et al. (2014) "Turbulent Flow Computation in a Circular U-Bend," EPJ Web of Conferences, vol. 67, 2014, p. 02075.

[15] M. Ayad Ali (2018) "CFD analysis for turbulent flow and heat transfer in U-tube," Journal of Engineering and Applied Sciences, vol. 13, pp. 11122-11134.

[16] N. Tran, C.C. Wang (2019) "Effects of tube shapes on the performance of recuperative and regenerative heat exchangers," Energy (Oxford), vol. 169, pp. 1-17.

[17] A. Gogolin, et al. (2020) "Influence of geometry and surface morphology of the U-tube on the fluid flow in the range of various velocities," Measurement: Journal of the International Measurement Confederation, vol. 164, p. 108094.

[18] N. Nikitin, A. Yakhot (2005) "Direct numerical simulation of turbulent flow in elliptical ducts," Journal of Fluid Mechanics, vol. 532, pp. 141-164.

[19] ANSYS Inc, (2013), ANSYS Fluent Theory Guide, U.S.A.